ISSN 1027-5495. Functional Materials, 25, No.4 (2018), p. 665-669.
doi:https://doi.org/10.15407/fm25.04.665 © 2018 — STC "Institute for Single Crystals"

# The peculiarities of the properties of $ZnS_xSe_{1-x}$ nanocrystals obtained by self-propagating high-temperature synthesis

***A.V.Kovalenko, Ye.G.Plakhtii, O.V.Khmelenko***

O.Honchar Dnipro National University, 72 Gagarina Ave.,
49010 Dnipro, Ukraine

*Received May 16, 2018*

$ZnS_xSe_{1-x}$ nanocrystals of all compounds were obtained by self-propagating high-temperature synthesis. It was found that the obtained samples had dimensions of 55±5 nm and were characterized by a mixed crystalline structure. With increase the $x$ value the fraction of the hexagonal phase in nanocrystals decreased from 65±5 % to 30±5 %, and the fraction of the cubic phase increased in the corresponding ratios. Despite the formation of $ZnS_xSe_{1-x}$ solid solutions, according to RCS data, the local environment of $Mn^{2+}$ impurity ions is not mixed. At a value of $0.2<x\leq1$, the $Mn^{2+}$ ions were surrounded by sulfur ions, and at $x\leq0.2$ it was surrounded by selenium ions. The change of the $Mn^{2+}$ ions local environment was accompanied by an abrupt change in the value of the RCS hyperfine structure of the $Mn^{2+}$ ions from $A = 6.88\div6.91$ mT to $A = 6.55$ mT. In $ZnS_xSe_{1-x}$ nanocrystals with $x = 1$ and $x = 0.9$, an EPR line with $g = 1.9998$ was detected, which is associated with an uncontrolled impurity — $Cr^+$ ions.

**Keywords**: $ZnS_xSe_{1-x}$ nanocrystals, self-propagating high-temperature synthesis, X-ray diffraction analysis, phases composition, crystalline structure, EPR spectrum.

Методом самораспространяющегося высокотемпературного синтеза получены нанокристаллы $ZnS_xSe_{1-x}$ всех составов размером 55±5 нм и характеризовались смешанной кристаллической структурой. С увеличением параметра $x$ доля гексагональной фазы в нанокристаллах уменьшалась с 65±5 % до 30±5 %, а доля кубической фазы возростала. По данным ЭПР локальное окружение примесных ионов $Mn^{2+}$ не является смешанным. При значении $0,2<x\leq1$ ионы $Mn^{2+}$ находились в окружении ионов серы, а при $x\leq0,2$ — в окружении ионов селена. В нанокристаллах $ZnS_xSe_{1-x}$ с $x = 1$ и $x = 0.9$ обнаружена линия ЭПР с $g = 1.9998$, которая связана с неконтролируемой примесью — ионами $Cr^+$.

**Особливості властивостей нанокристалів $ZnS_xSe_{1-x}$ отриманих методом самопоширюваного високотемпературного синтезу.** *О.В.Коваленко, Є.Г.Плахтій, О.В.Хмеленко.*

Методом самопоширюваного високотемпературного синтезу отримано нанокристали $ZnS_xSe_{1-x}$ всіх складів. Зразки мали розміри 55±5 нм і характеризувалися змішаною кристалічною структурою. Зі збільшенням параметра $x$ частка гексагональної фази у нанокристалах зменшується з 65±5 % до 30±5 %, а частка кубічної фази збільшується. За даними ЕПР локальне оточення домішкових іонів $Mn^{2+}$ не є змішаним. При значенні $0,2<x\leq1$ іони $Mn^{2+}$ знаходилися в оточенні іонів сірки, а при $x\leq0,2$ — в оточенні іонів селену. Зміна локального оточення іонів $Mn^{2+}$ супроводжувалася стрибкоподібною зміною параметра надтонкої структури ЕПР іонів $Mn^{2+}$ з величини $A = 6.88\div6.91$ mT до величини $A = 6.55$ mT. У нанокристалах $ZnS_xSe_{1-x}$ з $x = 1$ и $x = 0.9$ виявлено лінію ЕПР з $g = 1.9998$, яка пов'язана з неконтрольованою домішкою — іонами $Cr^+$.

## 1. Introduction

$ZnS_xSe_{1-x}$ solid solutions hold a specific place among semiconductor compounds of the $A_2B_6$–$A_2'B_6'$ type due to their physical properties. Depending on the value of $x$, such materials have an energy bandgap in the range 2.7÷3.7 eV that makes it possible to develop a short-wave radiation photosensitive devices, light-emitting diodes and lasers in the blue spectral band [1, 2]. In these days, additional attention to these compounds has been attracted by the common use of the $A_2B_6$ type of nanocrystals (NC) compounds in various optoelectronic-radiating structures [3]. This, in turn, stimulates the development of high-performance technologies for the production of NC with reproducible and controlled properties.

The self-propagating high-temperature synthesis (SHS) has several advantages among various methods for obtaining the $A_2B_6$ type of NC. This method is characterized by a high rate of NC production, the possibility to obtain the NC in large amounts, low cost and low energy consumption per unit, the simplicity of the applied equipment and its environmental compatibility [4]. The SHS method makes it possible to obtain $ZnS_xSe_{1-x}$ powdered NC by simple high-temperature reaction of Zn, S and Se fine powder mixture, to produce doped NC directly during the synthesis by adding the appropriate doping materials to the charge. It should be noted that ZnS NC [5], $ZnS:Mn^{2+}$ [6, 7], ZnSe polycrystals [8] were obtained earlier by the SHS method. However, according to our sources, the $ZnS_xSe_{1-x}$ and $ZnS_xSe_{1-x}$:Mn NC have not yet been synthesized by this method. In this study we analyze the peculiarities of $ZnS_xSe_{1-x}$ and $ZnS_xSe_{1-x}$:Mn NC obtaining by the SHS method, as well as the research results of their crystalline structures and EPR spectra.

## 2. Experimental

The NC synthesis of $ZnS_xSe_{1-x}$ and $ZnS_xSe_{1-x}$:Mn solid solutions were produced in a quartz vessel placed in a sealed steel reactor. The vessel was loaded with mechanically blended powders of Zn, S and Se taken at appropriate ratios. The premixing of the charge was carried out with the addition of ethyl alcohol to improve the mixing process. The S and Se ratio in the charge is characterized by the $x_p$ parameter. After drying of the mixture, the synthesis reaction was initiated by a thermal impulse that was provided by the nickel-chromium coil located in the upper part of the reactor. The synthesis was carried out at atmospheric pressure in the air. The S and Se ratio in the obtained $ZnS_xSe_{1-x}$ NC was determined by the $x$ parameter that, as further studies showed, differed from the $x_p$ parameter. Doping of the $ZnS_xSe_{1-x}$ NC with $Mn^{2+}$ ions was carried out by adding the $MnCl_2$ salt in an amount of $10^{-2}$ wt. % of the initial charge.

XRD analysis of the obtained NC was performed on a DRON-2 diffractometer using $CoK_\alpha$ radiation. The EPR spectra were studied using the Radiopan SE/X-2543 radiospectrometer. The images of nanoparticles were obtained using a scanning electron microscope REMMA-102-02.

## 3. Results and discussion

The $ZnS_xSe_{1-x}$ NC crystals obtained by SHS were a powder whose morphology is presented in Fig. 1a. The XRD data (Fig. 1c) demonstrate that this powder consisted of polycrystals with a mixed crystal structure and average sizes of 1–5 μm, while each polycrystal consisted of NCs. Their dimensions were determined by the Scherrer technique and were within 55±5 nm. The minimum dimensions of the $ZnS_xSe_{1-x}$ NCs were specific to the value $x = 0.2$, and the maximum for the compound with $x = 1$. The fraction of the hexagonal phase in the ZnS NC was ~ (65±5) %, the cubic phase ~ (35±5) %, in the $ZnS_{0.8}Se_{0.2}$ NC — (60±5) % and (40±5) %, in the $ZnS_{0.8}Se_{0.2}$ NC — (50±5) % and (50±5) %, and in the ZnSe NC — (30±5) % and (70±5) %, respectively. Thus, when the $x$ parameter decreases, the fraction of the cubic phase in the $ZnS_xSe_{1-x}$ NC increased. It is noteworthy that a large fraction of the hexagonal phase was present in the ZnSe NC that is not specific to the ZnSe bulk crystals. The parameters of the NC crystal lattice of $ZnS_xSe_{1-x}$ solid solutions in the cubic phase were in the range from $a = 5.386$ Å (for $x = 1$) to $a = 5.633$ Å (for $x = 0$). These values turned out to be smaller than the parameters of the crystal lattice of single crystals of $ZnS_xSe_{1-x}$ solid solutions [9], that are within $a = 5.4093$ (for $x = 1$) to $a = 5.6687$ Å (for $x = 0$). This, in turn, testifies the strain stresses specific to NC. The degree of microdeformations of the $ZnS_xSe_{1-x}$ ($\Delta a/a$) NC crystal lattice lies in the range from $5 \cdot 10^{-4}$ to $2 \cdot 10^{-3}$. The minimum degree of microdeformations was specific to compounds with $x = 1$ and $x = 0.9$, and the maximum — with $x = 0.2$.

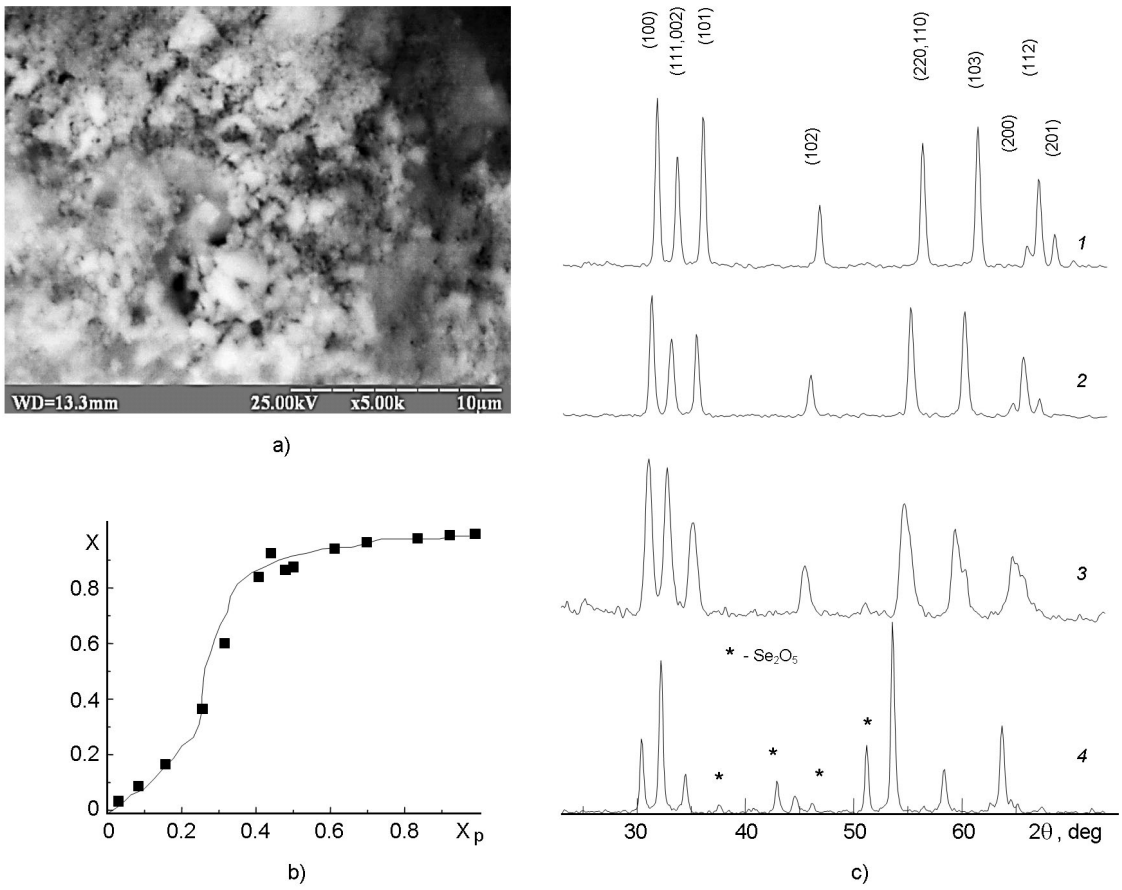


Fig. 1. The $ZnS_xSe_{1-x}$ NC surface morphology at $x = 0.8$; (a) dependence of the $x$ parameter in the $ZnS_xSe_{1-x}$ NC on the $x_p$ parameter; (b) XRD data; (c) NC: ZnS (*1*), $ZnS_{0.9}Se_{0.1}$ (*2*), $ZnS_{0.2}Se_{0.8}$ (*3*), ZnSe (*4*), $Se_2O_5$ phase is marked by * on X-ray diffraction patterns.

The dislocation densities ranged from $5 \cdot 10^{10}$ to $10^{12}$. The minimum dislocation density was specific to compounds with $x = 1$ and $x = 0$, and maximum for compounds with $x = 0.1$ and $x = 0.2$. The findings suggest that a large-scale rearrangement of the crystal lattice of the $ZnS_xSe_{1-x}$ NC occurs in the compound with $x = 0.2$.

Sediment consisting of selenium oxides was precipitated out on the walls of the reactor during the SHS reactions of the $ZnS_xSe_{1-x}$ NC at $x_p \leq 0.9$. This fact allows us to assume that the $x$ parameter in the $ZnS_xSe_{1-x}$ NC does not correspond to the $x_p$ parameter that determines the S and Se ratio in the charge prepared for SHS. To determine the $x$ parameter in the $ZnS_xSe_{1-x}$ NC as per XRD data, we used Vegard's law i.e. a linear variation of the crystal lattice parameters when the S and Se ratio is changed. Such a law is specific to crystals of $ZnS_xSe_{1-x}$ solid solutions [10]. As a result, it was found that in the synthesized $ZnS_xSe_{1-x}$ NC the parameter $x$ significantly differs from the $x_p$ parameter. The dependence between these parameters is shown in Fig. 1b.

According to the XRD data, the presence of other crystalline phases is not observed in the obtained solid solutions up to the compound with $x = 0$. Only in the ZnSe NC we detected the presence of the $Se_2O_5$ phase traces that is quite understandable in case of NC synthesis in the air. Here it should be noted that earlier in the study [11] when we obtained the ZnS NC by the SHS method, we observed the presence of $Mn_{0.75}Zn_{0.25}S$ phase. The dimensions of the NC were within 60±5 nm. The absence of this phase in these experiments can be explained by the fact that the SHS reaction was initiated by more powerful thermal pulse that provided by current nearly 35 Å, while in the study [11] it was nearly 27 Å. The findings indicate that the value of the initial thermal pulse in SHS affects both the dimensions of the NC and their phase composition that well within the results obtained by other authors [12].

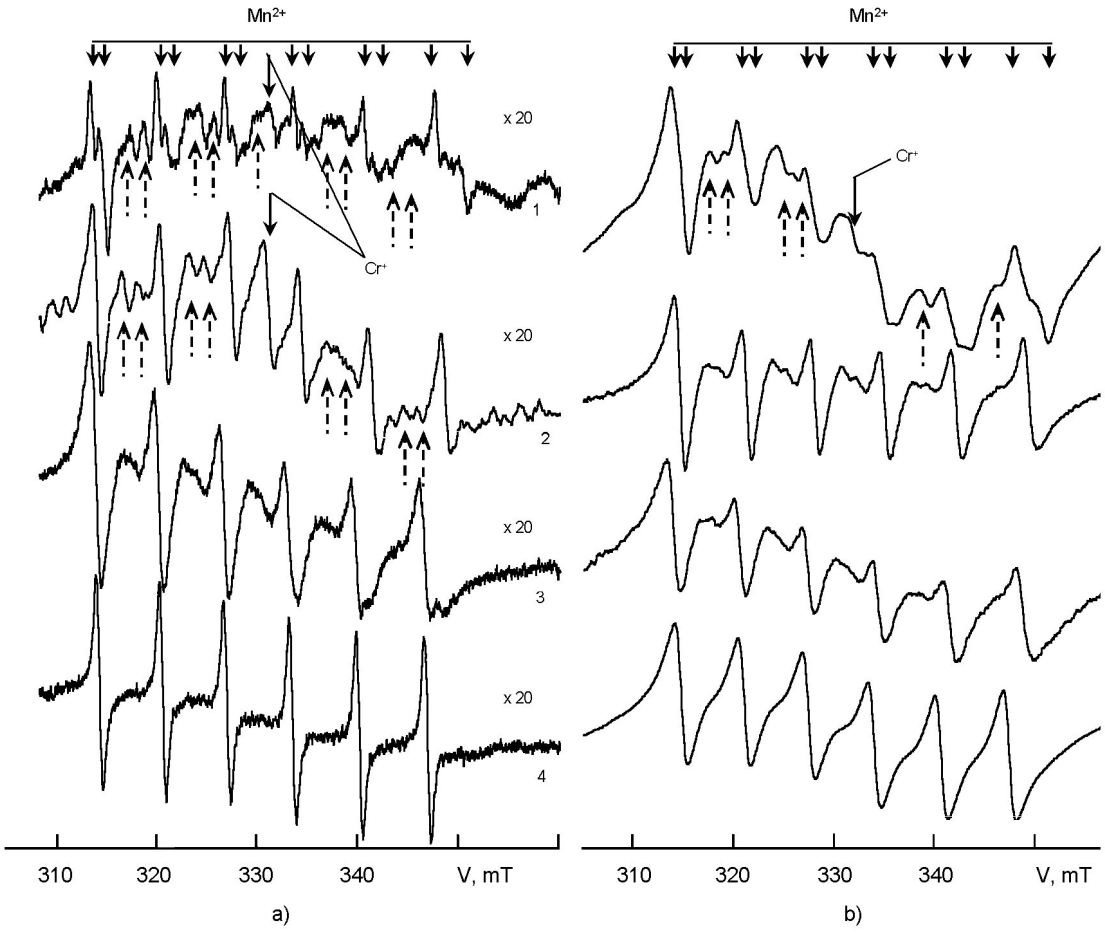


Fig. 2. EPR spectra of self-activated (a) NC: ZnS (*1*), $ZnS_{0.9}Se_{0.1}$ (*2*), $ZnS_{0.2}Se_{0.8}$ (*3*), ZnSe (*4*); EPR spectra of doped (b) NC:ZnS:Mn (*1*), $ZnS_{0.9}Se_{0.1}$:Mn (*2*), $ZnS_{0.2}Se_{0.8}$:Mn (*3*), ZnSe:Mn (*4*), dashed lines indicate forbidden transitions.

An investigation of the EPR spectrum of the $ZnS_xSe_{1-x}$ NC of solid solutions showed that, even in the NC undoped by manganese, all compounds contain a hyperfine structure consisting of six equidistant lines specific to the $Mn^{2+}$ paramagnetic centers (Fig. 2a). In the compound with $x = 1$, these lines turned out to be doubled that testify to overlapping of two EPR spectra. One of them, with the hyperfine structure constant $A = 7.15$ mT, belongs to the $Mn^{2+}$ ions located in a hexagonal local environment. Another spectrum, with a hyperfine structure constant $A = 6.88$ mT, is associated with $Mn^{2+}$ ions that are located in a cubic environment. The obtained result correlates with the XRD data that established the presence of a mixed crystal structure of the $ZnS_xSe_{1-x}$ NC. The weak lines are observed in the compounds with $x = 1$ and $x = 0.9$ (they are marked by dashed arrows in Fig. 2), that can be associated with forbidden transitions. For them, the change in the electron spin, as for the allowed transitions, is $\Delta M = \pm 1$, and the change of nuclear spin $\Delta m = \pm 1$, while for permissible transitions $\Delta m = 0$. The forbidden transitions were observed in the ZnS NC by other authors as well [13]. Their occurring is stipulated by severe lattice strain, as well as numerous disrupted bindings on the surface specific to NC. A single EPR line with $g = 1.9998$ associated with uncontrolled impurity — $Cr^+$ ions, was recorded in the same NC. Such line is also observed in ZnS bulk crystals [14]. It should be highlighted that usually the EPR signal stipulated by $Cr^+$ ions is detected in zinc sulphide crystals under UV excitation. The occurrence of such signal in unilluminated NC may indirectly indicate that the ZnS and $ZnS_{0.9}Se_{0.1}$ NC have the *n*-type of conductivity.

It is the electron capture at local levels of chromium that isovalently substitute the zinc in the zinc sulphide lattice ($Cr^{2+} + e = Cr^+$),

leads to the occurrence of a line associated with $Cr^+$ ions in the EPR spectra. At the room temperature, the EPR signal of $Cr^+$ ions in zinc selenide crystals is not observed due to the decrease in the spin-lattice relaxation time. In compounds with $0.2<x<0.9$, the EPR line with $g = 1.9998$ was also not observed. The intensity of forbidden transitions was found to be at the noise level, and one group of six hyperfine structure lines specific to cubic local symmetry in ZnS crystals dominated the EPR spectrum of $Mn^{2+}$ ions. For these compounds, the EPR ultrafine splitting constant of $Mn^{2+}$ ions varies insignificantly and is within the range of $A = 6.88 \div 6.91$ mT. Thus, it can be stated that in the NC of these compounds, the $Mn^{2+}$ ions are not placed in a mixed environment but in the environment of sulfur ions, although the XRD data indicate the presence of triple compounds in this range of $x$. In compounds where $x<0.2$, the crystal structure of $ZnS_xSe_{1-x}$ NC, as noted by the XRD data, is characterized by the maximum degree of microdeformations and the density of dislocations. According to EPR data, in these compounds the local environment of $Mn^{2+}$ ions changes abruptly, and now they are surrounded by selenium ions. The ultrafine splitting constant decreases abruptly to a value $A = 6.55$ mT. A similar result was observed in $ZnS_xSe_{1-x}$ bulk crystals [15].

The EPR spectrum of $ZnS_xSe_{1-x}$ NC doped by manganese is characterized by strong and wide lines of the hyperfine structure of $Mn^{2+}$ ions. Only in the compound with $x = 1$ this line structure is doubled (Fig. 2b), that confirms the presence of mixed crystal structure of ZnS NC. A single EPR line is observed in these crystals stipulated by $Cr^+$. In the compounds $0.9 \le x \le 1$, it is also possible to observe forbidden transitions with weak intensity. As in self-activated NC, despite the formation of mixed compounds according to XRD data, in $ZnS_xSe_{1-x}$ NC with $0.2<x\le1$, the $Mn^{2+}$ ions are not in a mixed environment but surrounded by sulfur ions. In compounds with $x \le 0.2$, simultaneously with the jump of the hyperfine structure constant, that was mentioned above, the local environment of $Mn^{2+}$ ions changes. In these NC, the $Mn^{2+}$ ions are surrounded by selenium ions.

Thus, the obtained results testify that it is possible to obtain NC of $ZnS_xSe_{1-x}$ mixed compounds by SHS method, as well as to dope them during the synthesis with a manganese admixture. A mixed crystal structure characterizes NC in all compounds. In the compounds with $0.2<x\le1$ according to the EPR data, the local environment of the $Mn^{2+}$ ions is not mixed. The $Mn^{2+}$ ions in these NC are surrounded by sulfur ions. In compounds with $x \le 0.2$, the $Mn^{2+}$ ions are surrounded by selenium ions. Simultaneously with the change in the local environment of $Mn^{2+}$ ions, the hyperfine structure constant of the EPR of $Mn^{2+}$ ions changes abruptly from a value $A = 6.88 \div 6.91$ mT to $A = 6.55$ mT. The presence of a single EPR line of $Cr^+$ ions in unilluminated $ZnS_xSe_{1-x}$ NC with $0.9 \le x \le 1$ can indirectly testify the $n$-type of the conductivity of the obtained samples.

## *References*


1. H.K.Sadekar, A.V.Ghule, R.Sharma, *J.Alloy. Compd.*, **509**, 18 (2011). DOI:10.1016/j.jallcom.2011.02.089
2. J.Lu, H.Liu, C.Sun et al., *Nanoscale*, **4**, 3 (2012). DOI:10.1039/C2NR11459C
3. D.V.Korbutiak, O.V.Kovalenko, S.I.Budzuliak, *Ukr. J. Phys. Rev.*, **7**, 1 (2012).
4. E.A.Levashov, A.S.Mukasyan, A.S.Rogachev, D.V.Shtansky, *Int. Mater. Rev.*, **62**, 4 (2016). DOI:10.1080/09506608.2016.1243291
5. S.V.Kozitskii, V.P.Pisarskii, O.O.Ulanova, *Combust. Explo. Shock.*, **34**, 1 (1998). DOI:10.1007/BF02606634
6. Y.Y.Bacherikov, N.P.Baran., I.P.Vorona et al., *J. Mater. Sci.-Mater. El.*, **28**, 12 (2017). DOI:10.1007/s10854-017-6580-8
7. N.E.Korsunska, Y.Y.Bacherikov, T.R.Stara et al., *Semiconductors*, **47**, 5 (2013). DOI:doi.org/10.1134/S1063782613050138
8. S.V.Kozytckyy, V.P.Pysarskyy, D.D.Polishchuk, *Phys. Chem. Sol. State*, **4**, 2 (2003).
9. T.Taguchi, Y.Kawakami, Y.Yamada, *Physica B*, **191**, 1 (1993). DOI:10.1016/0921-4526(93)90176-7
10. H.X.Chuo, T.Y.Wang, W.G.Zhang, *J.Alloy. Compd.*, **606** (2014). DOI:10.1016/j.jallcom.2014.04.004
11. M.F.Bulaniy, A.V.Kovalenko, A.S.Morozov, O.V.Khmelenko, *J. Nano Elect. Phys.*, **9**, 2 (2017). DOI:10.21272/jnep.9(2).02007
12. A.P.Amosov, I.P.Borovinskaya, A.G.Merzhanov, A.E.Sytschev, *Int. J. SHS*, **14**, 3 (2005).
13. P.A.Gonzalez Beermann, B.R.McGarvey, S.Muralidharan, R.C.Sung, *Chem. Mater.*, **16**, 5 (2004). DOI:10.1021/cm030435w
14. D.A.Reddy, G.Murali, R.P.Vijayalakshmi, B.K.Reddy, *Appl. Phys. A*, **105**, 119 (2011). DOI:10.1007/s00339-011-6563-1
15. M.F.Bulanyi, I.N.Geifman, T.A.Prokof'ev, A.N.Khachapuridze, *Inorg. Mater.*, **33**, 12 (1997).